Article

Dynamic Nature of the Transition State for the S1 Reaction Mechanism of Diphenylmethyl Acetates

Kevin S. Peters, Sarah Gasparrini, and Libby R. Heeb

J. Am. Chem. Soc., **2005**, 127 (37), 13039-13047• DOI: 10.1021/ja051219m • Publication Date (Web): 23 August 2005

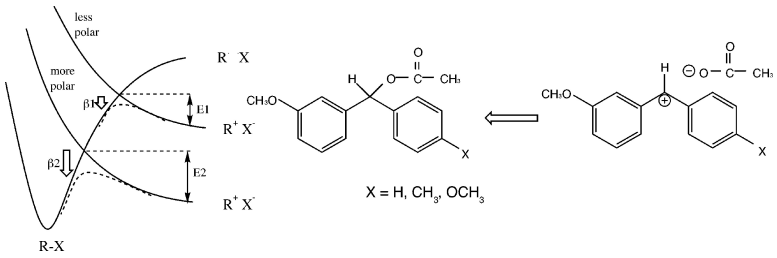

More About This Article

Additional resources and features associated with this article are available within the HTML version:

- Supporting Information
- Links to the 5 articles that cite this article, as of the time of this article download
- Access to high resolution figures
- Links to articles and content related to this article
- Copyright permission to reproduce figures and/or text from this article

View the Full Text HTML

J|A|C|S
ARTICLES
Published on Web 08/23/2005

Dynamic Nature of the Transition State for the S_N1 Reaction Mechanism of Diphenylmethyl Acetates

Kevin S. Peters,* Sarah Gasparrini, and Libby R. Heeb

Contribution from the Department of Chemistry and Biochemistry, University of Colorado, Boulder, Colorado 80309

Received February 25, 2005; E-mail: Kevin.Peters@Colorado.Edu

Abstract: Picosecond absorption spectroscopy is employed in the study of the reaction dynamics for the contact ion pairs produced upon the photolysis of a series of substituted diphenylmethyl acetates in the solvents acetonitrile, dimethyl sulfoxide, and 2,2,2-trifluoroethanol. From the temperature dependence of the rate constants, the activation parameters associated with covalent bond formation and diffusional separation to the solvent-separated ion pair are obtained. The activation parameters for bond formation are examined within the context of the Hynes theory for solvent dynamical effects on the passage through the transition state; deviations from the transition-state theory are found to be large. Factors that control nucleophilicity are discussed. Finally the validity of applying the Marcus equation to the S_N1 reaction mechanism is addressed.

Introduction

Since the initial formulation of the S_N1 reaction mechanism by Hughes and Ingold in the 1930s, elucidation of the parameters that control reactivity continues to be a topic of interest.[1−9] One long-sought goal is to correlate reactivity with structure. The standard approach for examining reactivity of reactions proceeding by the S_N1 mechanism has been to study the kinetics for reaction of resonance-stabilized cations with a variety of nucleophiles.[10] Study of these processes has led Ritchie to develop the N_+ scale.[11,12] More recently, Marcus theory has been employed in the correlation of rate constants with driving force, the analysis of which produces a fitting parameter identified as the intrinsic barrier.[13] The intrinsic barrier is thought to reflect the energies associated with desolvation of the nucleophile and the electrophile as well as electronic barrier for electrophile−nucleophile reaction.

The application of the Marcus theory to the analysis of electrophile−nucleophile combination has not met with universal acceptance. Ritchie has argued that the lack of identity reactions for electrophile−nucleophile reaction precludes defining an intrinsic barrier; the intrinsic barrier found in the correlation of the rate constant with the free-energy change for reaction is nothing other than a fitting parameter which cannot be given a precise physical interpretation.[14] However the general consensus of practitioners in the analysis of organic reactions kinetics within the context of the Marcus theory is that there is utility in deriving intrinsic barriers and that these barriers reflect something fundamental about the reaction process.[13,15−18]

In the present paper, we raise an issue regarding the applicability of Marcus theory, in its present analytical form, to the analysis of electrophile−nucleophile reaction that heretofore has not been directly addressed. A fundamental assumption in the current analytical form of Marcus theory is that the correlation of the rate constant with driving force for electrophile−nucleophile reaction assumes that the A factor is constant throughout a series of reactions, normally assigned a value of 6.6×10^{12} s^{-1} that is solvent independent.[13] Recently, we reported a series of experiments that examined the A factor for the reactions of chloride and the bromide ions with diphenylmethyl cation.[19,20] We found that the A factor for these reactions is less than that predicted by transition state theory and depends on the nature of the nucleophile as well as the solvent.

Diphenylmethyl chloride is an ideal molecular system for the study of the S_N1 reaction mechanism as each molecular event is kinetically resolved.[21−25] From our femtosecond and pico-

(1) Ingold, C. K. *Chem. Rev.* **1934**, *34*, 225−274.
(2) Winstein, S.; Clippinger, E.; Fainberg, A. H.; Robinson, G. C. *J. Am. Chem. Soc.* **1954**, *76*, 2597.
(3) Raber, D. J.; Harris, J. M.; Schleyer, P. v. R. *Ions and Ion Pairs in Organic Reactions*; Wiley: New York, 1974; Vol. 2.
(4) Doering, W. E.; Zeiss, H. H. *J. Am. Chem. Soc.* **1953**, *75*, 4733−4738.
(5) Raber, D. J.; Harris, J. M.; Schleyer, P. v. R. *J. Am. Chem. Soc.* **1971**, *93*, 4829−4833.
(6) Farcasiu, D.; Jahme, J.; Ruchardt, C. *J. Am. Chem. Soc.* **1985**, *107*, 5717−5722.
(7) Gajewski, J. J. *J. Am. Chem. Soc.* **2001**, *123*, 10877−10833.
(8) Bartl, J.; Steenken, S.; Mayr, H.; McClelland, R. A. *J. Am. Chem. Soc.* **1990**, *112*, 6918−6928.
(9) Minegishi, S.; Loos, R.; Kobayashi, S.; Mayr, H. *J. Am. Chem. Soc.* **2005**, *127*, 2641−2649.
(10) Ritchie, C. D. *Acc. Chem. Res.* **1972**, *5*, 348−354.
(11) Ritchie, C. D. *Acc. Chem. Res.* **1972**, *5*, 348−354.
(12) Mayr, H.; Kempf, B.; Ofial, A. F. *Acc. Chem. Res.* **2003**, *36*, 66−77.
(13) Richard, J. P.; Toteva, M. M.; Crugeiras, J. *J. Am. Chem. Soc.* **2000**, *122*, 1664−1674.
(14) Ritchie, C. D.; Kubisty, C.; Ting, G. Y. *J. Am. Chem. Soc.* **1983**, *105*, 279−284.
(15) Albery, W. J. *Ann. Rev. Phys. Chem.* **1980**, *31*, 227−263.
(16) Hine, J. *J. Am. Chem. Soc.* **1971**, *93*, 3701−3708.
(17) Guthrie, J. P. *J. Am. Chem. Soc.* **1991**, *113*, 7249−7299.
(18) Tsuji, Y.; Toteva, M. M.; Garth, H. A.; Richard, J. P. *J. Am. Chem. Soc.* **2003**, *125*, 15455−15465.
(19) Deniz, A. A.; Li, B.; Peters, K. S. *J. P. Chem.* **1995**, *99*, 12209−12213.
(20) Dreyer, J.; Lipson, M.; Peters, K. S. *J. Phys. Chem.* **1996**, *100*, 15162−15164.
(21) Peters, K. S.; Li, B. *J. Phys. Chem.* **1994**, *98*, 401−403.

Scheme 1

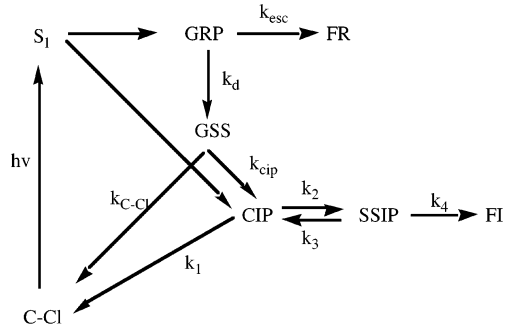

second studies of the reaction dynamics of the diphenylmethyl chloride geminate radical pair and the diphenylmethyl chloride contact ion pair, both produced upon the photolysis of diphenylmethyl chloride in acetonitrile, the reaction diagram shown in Scheme 1 is formulated.

On the 100-fs time scale, the first excited singlet state, S_1, decays by partitioning between the geminate radical pair, GRP, and the contact ion pair, CIP.[22] The transition to the GRP occurs along the excited-state surface through an adiabatic process; the GRP, in acetonitrile, is an excited-state product. The transition to the CIP is thought to pass through a conical intersection, which is a nonadiabatic process.[25] The GRP decays on the 100 picosecond time scale through two processes, diffusional separation to form free radicals (FR), k_{esc}, and a transition onto the ground-state surface (GSS), k_d, which partitions between ground-state reactant (C−Cl) and the CIP.[24] Whether the transition to the GSS should be modeled as a nonadiabatic electron-transfer process or be viewed as a passage through a conical intersection governed by Landau−Zener theory is still an open question.[22] The CIP decays through the formation of a covalent bond, k_1, or diffusional separation to the solvent-separated ion pair (SSIP), k_2. The SSIP then can either collapse reforming the CIP, k_3, or undergo further separation to free ions (FI), k_4. The transformation of FI → SSIP is not resolved. Each of the molecular processes envisioned by Winstein for the S_N1 reaction mechanism is now observed directly.[2]

In this study, we turn to the reaction dynamics associated with various substituted 3-methoxy-diphenylmethyl acetates so as to examine the nucleophilic character of the acetate ion. The *m*-methoxy system is chosen, as the photochemically induced yield of ion pairs is substantially larger than that produced upon the photolysis of diphenylmethyl acetate.[8,26] The enhanced yield from the *m*-methoxy substituent is another example of the meta effect first enunciated by Zimmerman.[27,28] We examine the reaction dynamics for the collapse of the CIP giving rise to covalent bond formation within the dynamical theory formulated by Hynes and co-workers.[29] The theory allows for the assessment of the dynamical nature of the system as it passes through the transition state. Questions regarding the strength of the coupling between the collapsing ions and the solvent are addressed. From the analysis, the electronic barrier associated with the S_N1 reaction mechanism is then obtained. Finally, the applicability of the Marcus theory for the analysis of the kinetics of covalent bond formation through the S_N1 reaction mechanism is assessed.

Experimental Section

The picosecond laser system employs a Continuum Leopard D-10 Nd:YAG laser with a pulse width of 10 ps. The optical detection system and the methods for data analysis have been described previously.[30] The samples were irradiated at 266 nm and probed at 440 nm for single wavelength measurements for the three cations. Transient spectra were obtained over the wavelengths of 400−650 nm for the three cations. The corresponding radicals do not absorb at 440 nm.[8]

The calculations of bond energies for homolysis and heterolysis are based upon B3LYP density functional theory at the 6-31G* level using Spartan 04.[31] The syntheses of 3-methoxy-diphenylmethyl acetate, 3-methoxy-4′-methyl-diphenylmethyl acetate, and 3,4′-dimethoxy-diphenylmethyl acetate are based on previous methods.[26]

The procedure for deriving the kinetic parameters depicted in Scheme 1 from the experimental kinetic data has been discussed previously.[21,23] Briefly, the time-dependent absorbance $A(t)$ obtained from the kinetic experiments results from the convolution of the instrument response function, $I(t)$ with the molecular kinetics, $F(t)$

$$A(t) = \int_{t-\infty} I(\tau)F(t-\tau)\,d\tau \qquad (1)$$

where the instrument response function $I(\tau)$ is the result of the convolution of the pump and probe beams and is assumed to have the analytical form of a Gaussian

$$I(t) = (2\pi\sigma)^{-0.5}\exp(-(t-t_0)/2\sigma^2) \qquad (2)$$

The parameters characterizing the Gaussian are obtained from the calibration compounds, pyrene and perylene. The kinetic model, $F(t)$, is described in ref 23 and contains the kinetic parameters k_d, k_1, k_2, k_3, and k_4. The five kinetic parameters are solved for simultaneously employing the downhill simplex method of Nelder and Mead for minization.[32] A fundamental assumption in the present analysis is that the extinction coefficients for the CIP, SSIP, and FI are the same at λ = 440 nm. This assumption is based upon observation that the absorption maximum for the diphenylmethyl cation, derived from the photolysis of diphenylmethyl chloride, does not shift as one pair evolves into another.[33] Within the resolution of the experimental apparatus, the same behavior is observed for each of the cations examined in the present study. Thus, the absorption spectra of the diphenylmethyl cation and the various substituted 3-methoxy-diphenylmethly cations are not sensitive to the presence of the counterion at the resolution of the experiment. This behavior contrasts with that of the fluorenyl ion pairs and the ketyl radical ion pairs which are sensitive to the counterion; a shift in the absorption spectrum is observed with the change in ion pair structure.[34,35]

Results

Kinetic Studies in Trifluoroethanol. The 266-nm irradiation of *m*-methoxy-diphenylmethyl acetate in 2,2,2-trifluroethanol

(22) Lipson, M.; Deniz, A. A.; Peters, K. S. *Chem. Phys. Lett.* **1998**, *288*, 781−784.
(23) Lipson, M.; Deniz, A. A.; Peters, K. S. *J. Phys. Chem.* **1996**, *100*, 3580−3586.
(24) Lipson, M.; Deniz, A. A.; Peters, K. S. *J. Am. Chem. Soc.* **1996**, *118*, 2992−2997.
(25) Dreyer, J.; Peters, K. S. *J. Phys. Chem.* **1996**, *100*, 15156−15161.
(26) McClelland, R. A.; Kanagasabapathy, V. M.; Steenken, S. *J. Am. Chem. Soc.* **1988**, *110*, 6913−6914.
(27) Zimmerman, H. E.; Somasekhara, S. *J. Am. Chem. Soc.* **1963**, *85*, 915−922.
(28) Zimmerman, H. E. *J. Am. Chem. Soc.* **1995**, *117*, 8988−8991.
(29) Zwan, G. v. d.; Hynes, J. T. *J. Chem. Phys.* **1982**, *76*, 2993−3001.
(30) Peters, K. S.; Lee, J. *J. Phys. Chem.* **1993**, *97*, 3761−3764.
(31) Hehre, W. J.; Yu, J.; Klunzinger, P. E.; Lou, L. *A Brief Guide to Molecular Mechanics and Quantum Chemical Calculations*; Wavefunction, Inc: Irvine, CA, 1998.
(32) Nelder, J. A.; Mead, R. *Comput. J.* **1965**, *7*, 308−313.
(33) Peters, K. S.; Li, B. *J. Phys. Chem.* **1994**, *98*, 401−403.
(34) Smid, J. In *Ions and Ion Pairs in Organic Reactions*; Szwarc, M., Ed.; Wiley: New York, 1972; Vol. 1, pp 85−152.
(35) Simon, J. D.; Peters, K. S. *J. Am. Chem. Soc.* **1983**, *105*, 4875.

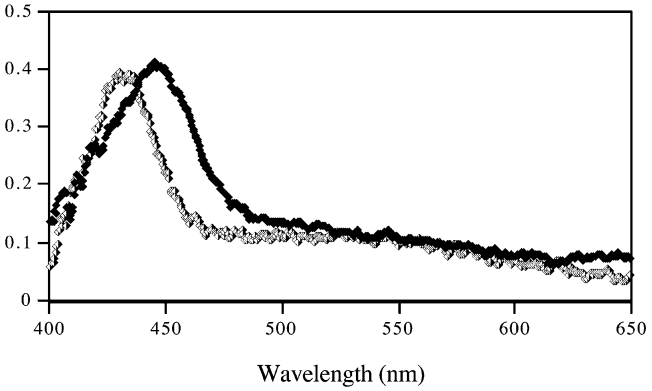

Figure 1. Transient absorption spectra following the 266-nm irradiation of 10 μM 3-methoxy-diphenylmethyl acetate (D+), open diamonds, and of 10 μM 3-methoxy-4′methyl-diphenylmethyl acetate (MethoxyD+), filled diamonds, in 2,2,2-trifluoroethanol, 23 °C at 100 ps.

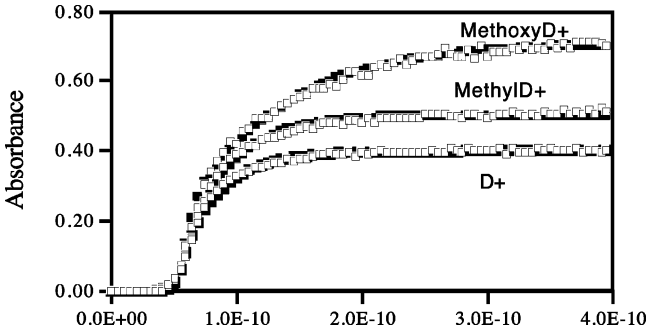

Figure 2. Dynamics of MethoxyD+, MethylD+, and D+ following the 266-nm irradiation of 10 μM 3,4′-dimethoxy-diphenylmethyl acetate, 10 μM 3-methoxy-4′-methyl-diphenylmethyl acetate, and 10 μM 3-methoxy-diphenylmethyl acetate in 2,2,2-trifluoroethanol at 23 °C. Open points are experimental data which are the average of four experiments. The solid calculated curve is based upon Scheme 1 with $t_0 = 75$ ps, pulse width $\sigma = 10$ ps, and $k_d = 3.3 \times 10^{10}$ s^{-1} for D+, $k_d = 2.7 \times 10^{10}$ s^{-1} for MethylD+, and $k_d = 1.4 \times 10^{10}$ s^{-1} for MethoxyD+.

(TFE) produces a transient absorption spectrum, with an absorption maximum at $\lambda = 435$ nm, Figure 1. The absorption profile is virtually identical to the absorption spectrum of the diphenylmethyl cation, whose absorption maximum is also at $\lambda = 435$ nm, and thus the transient species is assigned to the *m*-methoxy-diphenylmethyl cation (D+).[21] Similarly, the 266-nm irradiation of 3-methoxy-4′-methyl-diphenylmethyl acetate in TFE produces a transient species with an absorption maximum at $\lambda = 450$ nm, Figure 1. The *p*-methyl-diphenylmethyl cation has previously been observed with an absorption maximum at $\lambda = 450$ nm and thus again the transient species is assigned to the *m*-methoxy-*p*′-methyl-diphenylmethyl cation (MethylD+).[36] Finally the 266-nm irradiation of 3,4′-dimethoxy-diphenylmethyl acetate in TFE also produces a transient species absorbing at $\lambda = 450$ nm, which is assigned to the *m*,*p*′-dimethoxy-diphenylmethyl cation (MethoxyD+). During the time evolution of the transient absorption spectrum for each of the three species, the absorption maximum does not shift.

The kinetic behaviors of the three cations, D+, MethylD+, and MethoxyD+ in TFE are probed at 440 nm over the time course of 400 ps, Figure 2. The kinetics for the appearance of each the three cations is biphasic. The first components for the appearance of each of the cations occurs within the laser pulse

(36) Olah, G. A.; Pittman, C. U.; Symons, M. C. R. In *Carbonium Ions*; Olah, G. A., Schleyer, P. v. R., Eds.; John Wiley & Sons: New York, 1970; Vol. 1, pp 154−217.

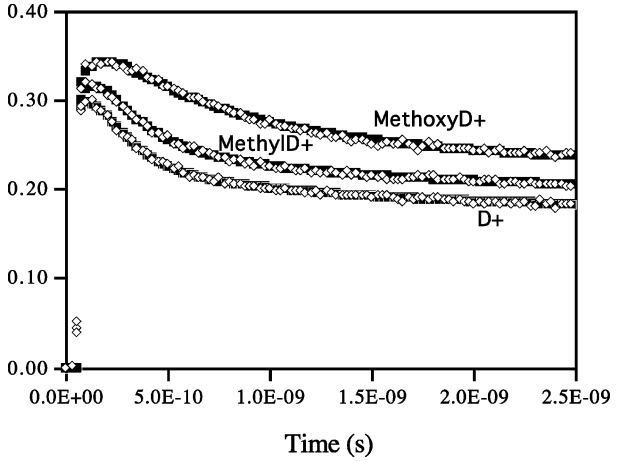

Figure 3. Dynamics of MethoxyD+, MethylD+, and D+ following the 266-nm irradiation of 10 μM 3,4′-dimethoxy-diphenylmethyl acetate, 10 μM 3-methoxy-4′-methyl-diphenylmethyl acetate, and 10 μM 3-methoxy-diphenylmethyl acetate in acetonitrile at 23 °C. Open points are experimental data which are the average of four experiments. The solid calculated curve is based upon Scheme 1 and the rate constants given in Table 1 with $t_0 = 75$ ps, pulse width $\sigma = 10$ ps, and $k_d = 1.1 \times 10^{10}$ s^{-1} D+, $k_d = 1.1 \times 10^{10}$ s^{-1} for MethylD+, and $k_d = 1.0 \times 10^{10}$ s^{-1} for MethoxyD+.

and thus are not kinetically resolved. However, the second components are resolved; the second component for D+ appears with a rate constant of 3.3×10^{10} s^{-1}, while the corresponding rate constant for MethylD+ is 2.7×10^{10} s^{-1} and for MethoxyD+ is 1.4×10^{10} s^{-1}. In TFE, there is no measurable decay of the cations onto 4 ns time scale.

By application of Scheme 1 to the analysis of the reaction dynamics of the three acetates, the biphasic appearance of the corresponding cations can be understood as arising by two processes. The fast component is associated with the decay of the excited singlet state to produce a CIP as is observed in the decay of the diphenylmethyl chloride excited singlet state.[22] The second component is associated with the decay of the GRP to give rise to the CIP, a process also observed in the diphenylmethyl chloride radical pair.[22] The kinetics of the decay of the GRP are governed by two processes: a nonadiabatic transition to GSS, k_d, and diffusional separation of the radical pair, k_{esc}, Scheme 1. Thus, the second component of the biphasic kinetics reflects the decay of the GRP onto the GSS leading to the formation of the CIP. To obtain the rate constants for both conversion onto GSS, k_d, and diffusional separation to form FR, k_{esc}, the dynamics of the GRP must be monitored directly. This will be a subject for future investigation.

Kinetic Studies in Acetonitrile. The kinetic behaviors of the contact ion pairs for D+, MethylD+, and MethoxyD+ in acetonitrile, monitored at $\lambda = 440$ nm, are shown in Figure 3; the transient absorption spectra of the three species are virtually identical to those in TFE. To accurately account for the observed dynamics, the kinetic model depicted in Scheme 1 is employed. In particular, the decay of the GRP to give rise in the CIP, k_d, must be taken into account; exclusion of this reaction pathway does not give an acceptable fit of the model to the kinetic data. Also, the interconversion between CIP, SSIP, and FI must be included into the model for an acceptable fit of the model to the experimental data. The fitting parameters associated with Scheme 1 are given in Table 1.

The temperature dependencies for covalent bond formation, k_1, as well as the diffusional separation to the SSIP, k_2, are

Table 1. Kinetic Parameters from Scheme 1 for the Ion Pair Dynamics Associated with D+, MethylD+, MethoxyD+, DPMC, and DPMB in Acetonitrile at 23 °C

compound	k_1 ($\times 10^9$cs^{-1})[a]	k_2 ($\times 10^9$ s^{-1})	k_3 ($\times 10^8$ s^{-1})	k_4 ($\times 10^8$ s^{-1})
D+	3.0	3.5	4.0	8.0
MethylD+	2.2	3.0	3.9	8.0[b]
MethoxyD+	0.6	1.3	3.9	8.0[b]
DPMC[d]	3.8	2.9	1.31	7.8
DPMB[e]	3.2	5.6	*c*	c

[a] Uncertainties in fits are ±10%. [b] Values obtained in the fits of D+ where held constant. [c] Can not be resolved. [d] Taken from ref 19. [e] Taken from ref 20.

Table 2. Activation Parameters, A Factor, and E_a from Arrhenius Analysis of k_1 for Covalent Bond Formation from Collapse of CIP and k_2, Decay of CIP into SSIP in the Solvents Acetonitrile and Dimethyl Sulfoxide

solvent			D+	MethylD+	MethoxyD+
CH_3CN	k_1	E_a (kcal/mol)[b]	1.9	3.2	5.4
		A ($\times 10^{12}$ s^{-1})[c]	0.075	0.51	5.5
	k_2	E_a (kcal/mol)[b]	1.0	1.1	1.5
		A ($\times 10^{12}$ s^{-1})[c]	0.011	0.023	0.06
DMSO	k_1	E_a (kcal/mol)[b]	a	3.5	2.8
		A ($\times 10^{12}$ s^{-1})[c]	a	1.9	0.14
	k_2	E_a (kcal/mol)[b]	a	2.3	1.9
		A ($\times 10^{12}$ s^{-1})[c]	a	0.13	0.05

[a] Can not be determined. [b] Estimated error ±20%. [c] Estimated error ±50%.

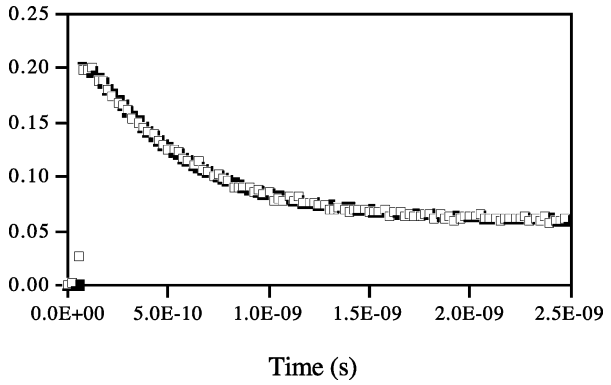

Figure 4. Dynamics of MethoxyD+, following the 266-nm irradiation of 10 μM 3,4′-dimethoxy-diphenylmethyl acetate in dimethyl sulfoxide at 23 °C. Open points are experimental data that are the average of four experiments. The solid calculated curve is based upon Scheme 1 and the rate constants given in Table 3 with $t_0 = 75$ ps, pulse width $\sigma = 10$ ps, and $k_d = 5 \times 10^{10}$ s^{-1}.

examined over the temperature range of 14−47 °C; data at nine temperatures are obtained for each CIP. An Arrhenius analysis of the temperature dependence of k_1 and k_2 produces the activation parameters, A and E_a, which are shown in Table 2.

Kinetic Studies in Dimethyl Sulfoxide. The ion-pair dynamics of MethoxyD+ in dimethyl sulfoxide, monitored at 440 nm, are shown in Figure 4; the transient absorption spectra of the three species are virtually identical to those in TFE. The fitting parameters associated with the application of Scheme 1 in the analysis of the kinetic data are given in Table 3. Similar behavior for MethylD+ in dimethyl sulfoxide is found whose fitting parameters are also given in Table 3. When the decay of the ion pair for D+ is examined in dimethyl sulfoxide, Figure 5, application of the kinetic model associated with Scheme 1 cannot be fit to the experimental data. In particular, at early times, there is a rapid decay of the CIP during the first 50 ps that cannot be fit to the model and thus the fitting parameters

Table 3. Kinetic Parameters from Scheme 1 for the Ion Pair Dynamics Associated with MethylD+ and MethoxyD+ in Dimethyl Sulfoxide at 23 °C

compound	k_1 ($\times 10^9$ s^{-1})[a]	k_2 ($\times 10^9$ s^{-1})	k_3 ($\times 10^8$ s^{-1})	k_4 ($\times 10^8$ s^{-1})
MethylD+	4.8	2.6	2.5	8.0
MethoxyD+	1.7	0.7	2.5	8.0[b]

[a] Uncertainties in fits are ±10%. [b] Values obtained in the fits of MethylD+ where held constant.

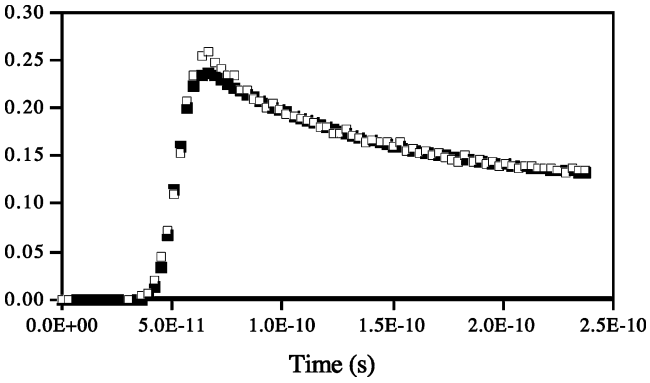

Figure 5. Dynamics of D+, following the 266-nm irradiation of 10 μM 3-methoxy-diphenylmethyl acetate in dimethyl sulfoxide at 23 °C. Open points are experimental data that are the average of four experiments. The solid calculated curve is based upon Scheme 1 and $k_1 = 6.9 \times 10^9$ s^{-1} with $t_0 = 65$ ps, pulse width $\sigma = 10$ ps, and $k_d = 5 \times 10^{10}$ s^{-1}. The lack of an acceptable fit is due to time-dependent kinetics.

Table 4. Energies for Bond Homolysis and Bond Heterolysis of Substituted Diphenylmethyl Acetates, Chloride,s and Bromide in Acetonitrile

compound	homolysis (kcal/mole)	heterolysis (kcal/mole)
diphenylmethylactetate	58.7	32.2
3-methoxy-	59.1	30.8
3-methoxy-4′-methyl-	59.0	27.0
3,4′-dimethoxy-	58.9	21.3
DPMC	61.8	27.4
DPMB	46.0	21.8

for D+ are not given in Table 4. This kinetic behavior is indicative of a time-dependent kinetic process.[37] This behavior will be addressed in the Discussion.

The parameters from the Arrhenius analysis of the temperature dependencies of the collapse of the CIPs for MethoxyD+ and MethylD+ in dimethyl sulfoxide resulting in covalent bond formation, k_1, and CIP separation, k_2, over the range of 23−53 °C, are given in Table 2.

Radical-Pair and Ion-Pair Energies. Since the energies associated with the radical pairs and ion pairs encountered in the present kinetic study have not been experimentally determined, an estimate is established through the analysis of a series of thermodynamic cycles. We begin by considering the experimentally determined gas-phase homolytic bond dissociation energy of benzyl acetate.[38]

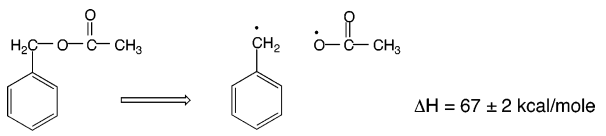

(37) Northrup, S. H.; Hynes, J. T. *J. Chem. Phys.* **1978**, *69*, 5246−5260.
(38) McMillen, D. F.; Golden, D. R. *Annu. Rev. Phys. Chem.* **1982**, *33*, 493−526.

From the isodesmic reaction calculated at the B3LYP/6-31G* level, the homolytic bond dissociation energy of diphenylmethyl acetate is derived.

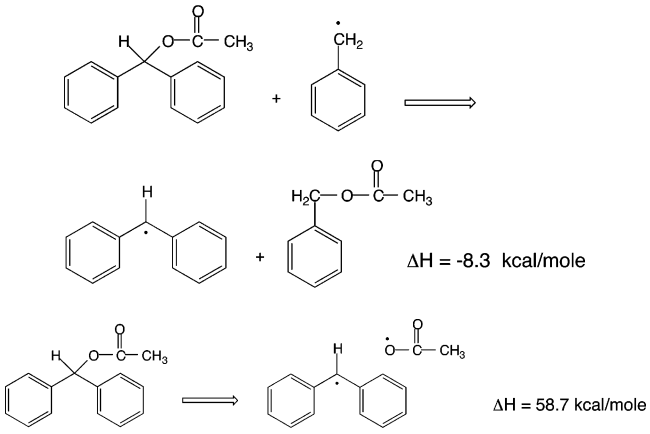

The energy of the diphenylmethyl cation/acetate ion pair is estimated from the oxidation potential of the diphenylmethyl radical, $E_{1/2}^{ox}$ (SCE/CH_3CN) +0.35 V, and from the oxidation potential of the acetate ion, $E_{1/2}^{ox}$ (SCE/CH_3CN) +1.5 V, assumed to be reversible, to give the energy of bond heterolysis in acetonitrile.[39] The energy for the formation of the contact ion pair should be of the order of 1 kcal/mol and thus is ignored.[40]

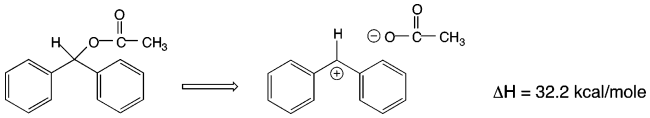

The energies of the various substituted diphenylmethyl acetate radical pairs are determined through a series of isodesmic reactions, again calculated at the B3LYP/6-31G* level, the results of which are given in Table 4.

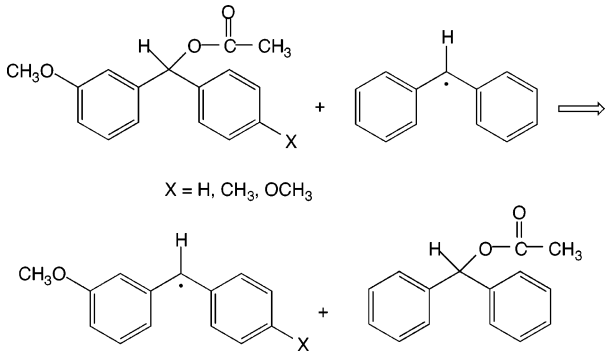

The same procedure is used to determine the energies of the various substituted diphenylmethyl acetate contact ion pairs, Table 4. Finally, the energies for homolysis and heterolysis for diphenylmethyl chloride and diphenylmethyl bromide in acetonitrile, determined by the same protocol, are given in Table 4.[38,39]

Discussion

Reactions in Acetonitrile. The standard theoretical model employed in the analysis of the kinetics for reactions proceeding through the S_N1 reaction mechanism is transition-state theory.[41]

$$k_{TST} = (k_b T/h) \exp(-\Delta G^{\ddagger}/k_b T) \quad (3)$$

In recent years, the focus of analysis for such reactions has been on the relationship between activation free energy $\Delta G^{\ddagger}$ and the driving force ΔG.[15] A fundamental assumption for this form of transition-state theory is that the solvent and the charged species in the region of the transition state are always equilibrated with one another as the reaction progresses. The influence of solvent is found only in the static effect upon the potential of mean force. The dynamical aspect of solvation is not taken into account.

When a charged species passes through the transition state, the movement of charge will induce a polarization in the surrounding solvent molecules producing a retarding force by the solvent on the charged reactants. The strength of the interaction between the charged molecular species and the solvent as well as the relaxation time of the solvent about the charged species should have a strong influence upon the overall reaction dynamics. These considerations led Hynes and co-workers to develop a theory for the dynamical coupling between solute and solvent for reacting systems.[29]

Employing the Langevin model as the description for the reaction dynamics of charged species traversing the transition state, Hynes and co-workers addressed the nature of the coupling between the charged solute and the solvent.[29] In the transition state, the reacting species experiences two forces. The first is due to the potential of mean force, the reaction barrier, ω_b; this force drives the reacting species off of the transition state toward product. In opposition is the force exerted by the solvent produced by the movement of charged species off of the transition state. In the Langevin model, the solvent force is manifested as a time-dependent friction, $\zeta(t)$, exerted upon the reacting species, and associated with the solvent force is an electrostatic solvent frequency, ω_s. If ω_s is less than ω_b, then the effect of the interaction of the solvent with the solute is to retard the solute movement off of the transition state. This drag will reduce the rate of passage through the transition state, but the reacting species can still evolve into product without relaxation of the solvent. A measure of the deviation from the prediction of transition state theory can be found in the transmission coefficient κ defined as the ratio of the prefactors from the Arrhenius equation and from transition state theory.[19] Model calculations reveal that the reduction in the rate constant k relative to that predicted by transition state theory, k_{TST}, is small with a range in κ from 0.8 to 1.0.[29] Solvent dynamics do not have a profound effect upon the rate for reaction. The regime where $\omega_s < \omega_b$ is in the limit of "nonadiabatic solvation". In the opposite regime where $\omega_s > \omega_b$, the forces exerted by the solvent dominate the reaction barrier force and the reacting species cannot move off of the transition state until the solvent relaxes. The time scale identified as characterizing the solvent relaxation is τ_l, the longitudinal relaxation time. During this time period, there will be multiple recrossings of the transition state by the reacting species significantly reducing the rate constant k from the prediction of transition state theory which assumes as single crossing. Model calculations suggest that $\kappa < 0.1$ can be achieved; the rate constant for reaction can be an order of

(39) Wayner, D. D. M.; McPhee, D. J.; Griller, D. *J. Am. Chem. Soc.* **1988**, *110*, 132−137.
(40) Arnold, B. R.; Farid, S.; Goodman, J. L.; Gould, I. R. *J. Am. Chem. Soc.* **1996**, *118*, 5482−5483.
(41) Kim, H. J.; Hynes, J. T. *J. Am. Chem. Soc.* **1992**, *114*, 10508−10528.

magnitude less than that predicted by transition state theory but how much less has yet to be established by experiment. The regime where $\omega_s > \omega_b$ is the "polarization caging" limit.[29]

To establish κ, a model for k_{TST} is required. For the S_N1 reaction mechanism, Hynes and co-workers proposed the following form for the collapse of a CIP to form a covalent bond[42]

$$k_{TST} = (\omega^R/2\pi)(\omega_s(R)/\omega_s(r^\dagger))(Q_{rot}(r^\dagger)/Q_{rot}(R)) \times \exp(-\Delta G^\dagger/k_B T) \quad (4)$$

The solvent frequencies associated with the fluctuation of the solvent forces about the CIP and the transition state are $\omega_s(R)$ and $\omega_s(r^\dagger)$, respectively. The geometries are manifested in the rotational partition functions for the CIP and the transition state, $Q_{rot}(R)$ and $Q_{rot}(r^\dagger)$. $\Delta G^\ddagger$ represents the difference in the equilibrium potential of mean force for the CIP and the transition state. Finally, ω^R is the vibrational frequency associated with the CIP whose motion moves the system into the transition state.

One of the great difficulties in determining k_{TST} is the lack of methodology for establishing the solvent frequencies $\omega_s(R)$ and $\omega_s(r^\dagger)$ associated with the fluctuation of the solvent forces about the CIP and the transition state.[19] Also, the ion-pair frequency, ω^R, associated with the reaction coordinate has not been measured, although in principle is obtainable. In our prior analysis of the transition-state rate constant for the collapse of the diphenylmethyl chloride CIP and the diphenylmethylbromide CIP, we were forced to employ the values for $\omega_s(R)$ and $\omega_s(r^\dagger)$ obtained by Hynes and co-workers from their theoretical modeling of the S_N1 reactions of *tert*-butylchloride and *tert*-butylbromide.[19] The CIP vibrational frequency ω^R was estimated based upon the vibrational frequencies of inorganic salts. The estimated values for the frequency factors from transition state theory for diphenylmethyl chloride and diphenylmethylbromide are 5.7 and 3.3×10^{12} s^{-1}, respectively. However, given the uncertainty in ascertaining the value of the parameters in eq 4, this procedure for determining the frequency factors is clearly problematic.

One of the principle aims of the present study is to determine the degree of breakdown of transition-state theory as measured by κ. Recognizing that the A factor for any reaction in solution will always be equal to or less than the frequency factor derived from transition-state theory, comparison of A factors for a series of reactions will yield an upper bound for κ. This is illustrated by considering the series of A factors for reactions in acetonitrile, Table 2. Taking the A factor for MethoxyD+, 5.5×10^{12} s^{-1}, as the upper limit for the frequency factor, the κ value for MethylD+ is 0.09 while the κ value for D+ is 0.013. Setting an upper bound to 5.5×10^{12} s^{-1} then allows us to circumvent establishing an upper limit based upon theoretical modeling as was done in prior studies.[19,20] For D+, the passage through the transition state is reduced by a factor of 77 relative to MethoxyD+, due to multiple recrossing of the transition state, which places the dynamics for the collapse of D+ and acetate ion to form a covalent bond in the polarization caging regime. It is the evolution of the solvent structure about the reacting species that controls the passage through the transition state. For comparison, the values of κ for the collapse of the diphenylmethyl chloride CIP and the diphenylmethylbromide CIP in acetonitrile are 0.16 and 0.15, both in the polarization caging regime.

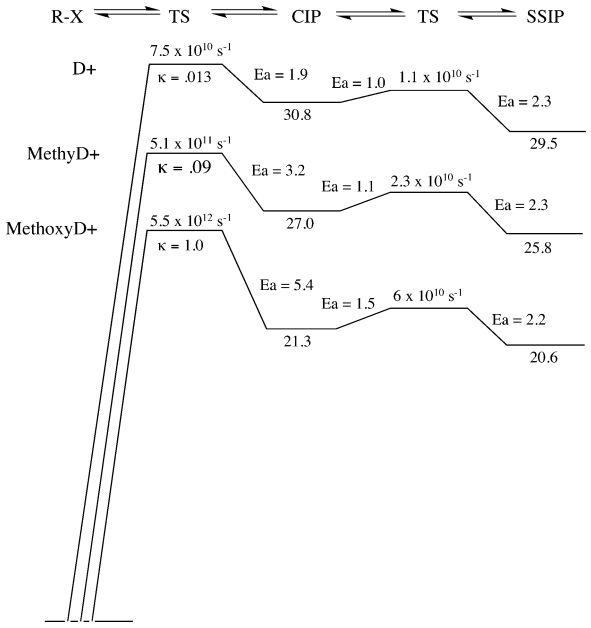

Figure 6. Reaction profile for D+, MethylD+, and MethoxyD+ in acetonitrile based on data from Table 1 and Table 2.

From the temperature-dependent studies of k_1 and k_2 and the determination of the energies of the ionic intermediates, Table 4, the reaction profile for D+, MethylD+, and MethoxyD+ in acetonitrile is constructed, Figure 6. From the rate constants k_2 and k_3, the free-energy changes for the transformation of the SSIP into the CIP are calculated; ΔG (SSIP → CIP) = 1.3 kcal/mol for D+, ΔG (SSIP → CIP) = 1.2 kcal/mol for MethoxyD+, and ΔG (SSIP → CIP) = 0.7 kcal/mol for MethoxyD+. It is important to note that, in Figure 6, the energy change associated with R−X → CIP is a change in enthalpy while the energy change associated with CIP→ SSIP is a change in free energy. The free-energy change for R−X → CIP cannot be determined due to our inability to determine the entropy change for this process. For the collapse of the CIP giving rise to bond formation (R−X), the energy of activation increases with increasing stability of the CIP. There is also a correlation of the decrease in the energy of activation with a decrease in the A factor. Presumably, in acetonitrile, as the energy of activation decreases, the curvature of the potential of mean force decreases, leading to a decrease in ω_b. In turn, solvent forces reflected in ω_s increasingly dominate the dynamics of the passage through the transition state causing an increasing breakdown of transition-state theory. For the reactions of D+ and MethylD+ with the acetate ion, the dynamics fall within the polarization caging limit; solvent relaxation controls the passage through the transition state.[19] On the other hand, MethoxyD+ is placed in the nonadiabatic solvation regime where the effect of solvent is to retard transition-state passage.

On the basis of the data obtained in prior studies, the energies for the reaction profile and the associated activation parameters for diphenylmethyl chloride (DPMC) and diphenylmethyl bromide (DPMB) are shown in Figure 7.[19,20] The value for κ is based on the determination of k_{TST} employing eq 4. For DPMB, the rate constants for decay of the SSIP, k_3 and k_4, could not be

(42) Kim, H. J.; Hynes, J. T. *J. Am. Chem. Soc.* **1992**, *114*, 10528−10537.

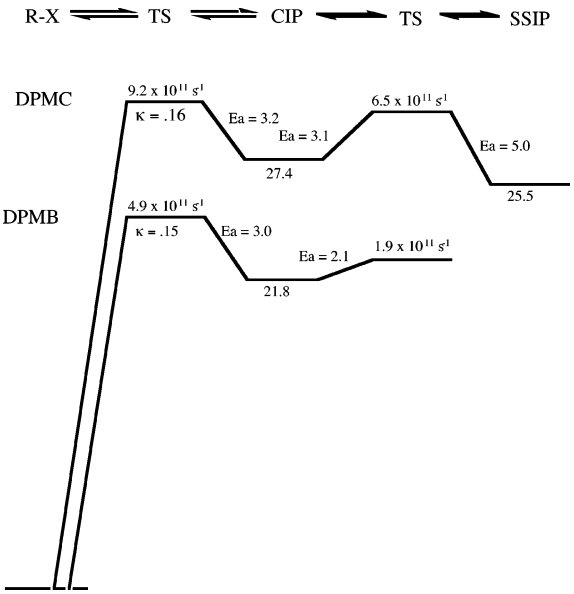

Figure 7. Reaction profile for DPMC and DPMB in acetonitrile based on data from refs 19 and 20.

resolved and thus it is not possible to determine the free energy change for the transformation of the SSIP into the CIP.

Reactions in Dimethyl Sulfoxide. Two aspects of the kinetic data for reactions occurring in dimethyl sulfoxide require comment. The first is the nature of the reaction dynamics for D+. The decay of D+ through recombination with the acetate ion is time dependent; the kinetics cannot be fit to a time-independent model, Figure 5. At early times in the decay process, the rate of recombination is faster than at later times. Figure 5 displays the fit of the model, Scheme 1, assuming that k_1 is 6.9×10^9 s^{-1}. This rate constant is substantially larger than the rate constant for D+ recombining with the acetate ion in acetonitrile, $k_1 = 3.0 \times 10^9$ s^{-1}, whose kinetic data is fit to a time independent rate constant. The faster decay in dimethyl sulfoxide must then reflect a smaller electronic barrier. A rationalization of the time-dependent behavior can be found in works of Hynes.[37] At any given instance, there will be a distribution of solvent structures surrounding the reacting species. A subset of these structures may allow the reacting species to evolve into product. Once this population is depleted, further product formation will occur only with the redistribution in solvent structures. If reaction of the initial substructure is faster than the solvent redistribution time due to a small electronic barrier, solvent reorganization will govern further reaction dynamics and thus the kinetic profile will be time dependent. Such behavior is not observed in acetonitrile, which is accounted for by a larger electronic barrier and faster solvent reorganization. Maroncelli and co-workers measured, through time-resolved emission studies, the solvent-relaxation dynamics for numerous solvents about the excited state of coumarin 153.[43] Acetonitrile has two time scales associated with its relaxation, 0.089 and 0.63 ps. In contrast, dimethyl sulfoxide has three time components, 0.214, 2.29, and 10.7 ps. If the long time-scale components of the solvent reorganization are important in establishing the redistribution of solvent structures about the reacting species that allow for reaction, then the reorganization

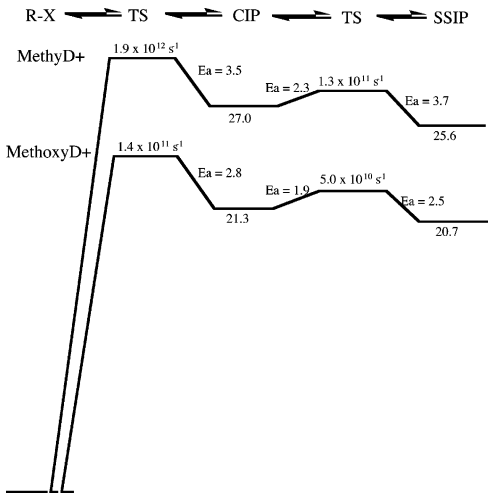

Figure 8. Reaction profile for MethylD+ and MethoxyD+ in dimethyl sulfoxide based on data from Tables 2 and 3.

Scheme 2

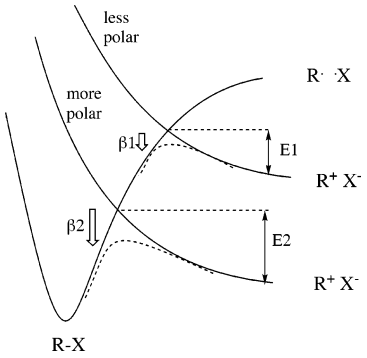

in dimethyl sulfoxide is a factor of 17 slower than acetonitrile. It may be the slow response of the solvent that leads to the time-dependent phenomenon found in Figure 5.

The reaction profile for the recombination of MethylD+ and MethoxyD+ with acetate in dimethyl sulfoxide is shown in Figure 8. The energies of the CIP are assumed to be the same as those found in acetonitrile. On the basis of the Onsager dipole solvation model, an increase in dielectric constant from $\epsilon = 37.5$ (acetonitrile) to $\epsilon = 46.6$ (dimethyl sulfoxide) will produce only a very small change in the energy of the CIP.[40] Most surprising is that, as the energy of the CIP decreases on going from MethylD+ to MethoxyD+, the electronic barrier for covalent bond formation decreases, a trend opposite to that found for the reactions in acetonitrile. It has been a central tenant of organic reactivity, excluding electron and proton transfer, that as the driving force decreases for a series of analogous reactions, the electronic barrier for reaction should increase.[44] To understand the possible origin of this effect we turn to the theoretical formalism developed by Hynes and co-workers for the S_N1 reaction mechanism.[41]

The potential energy diagrams for the S_N1 reaction mechanism are based upon valence bond approach, Scheme 2.[41,45] In the gas phase, the ground-state diabatic surface correlates with the covalent bond R−X dissociating into the radical pair, R···X. The excited singlet-state diabatic surface for the system

(43) Horng, M. L.; Gardecki, J. A.; Papazyan, A.; Maroncelli, M. *J. Phys. Chem.* **1995**, *99*, 17311−17337.

(44) Hammond, G. S. *J. Am. Chem. Soc.* **1955**, 334−338.
(45) Pross, A.; Shaik, S. S. *Acc. Chem. Res.* **1983**, *16*, 363.

correlates with the ion pair R^+X^-. In polar solvents, the R^+X^- diabatic surface falls below the R···X diabatic surface as the separation between R and X increases.

Hence along the bond-stretch coordinate there is a crossing between the two diabatic surfaces in polar solvents. At the crossing, there will be a mixing of the two states due to their electronic coupling, $\beta(r)$, which is distance dependent. From the perspective of the CIP collapsing to form R−X, as the CIP stability increases relative to R−X, the position of the diabatic state curve crossing moves toward R−X, which in itself should give rise to a larger electronic barrier as the barrier moves toward R−X, E2 > E1. However, as the curve crossing moves toward R−X, the electronic coupling $\beta(r)$ also increases, $\beta 2 > \beta 1$, which serves to reduce the electronic barrier. Hynes and coworkers found that, as the curve crossing moves toward R−X, $\beta(r)$ increases in a highly nonlinear manner, which can more than offset the increase in electronic barrier due to curve crossing as the stability of CIP increases relative to R−X.[41] Again from the CIP → R−X perspective, there will be regimes where the increase in stability of CIP relative to R−X gives rise to an increase in the energy of the transition state relative to CIP and other regimes there will be a decrease in the energy of the transition state relative to CIP. The demarcation of these two regimes will be a sensitive function of the nature of the two diabatic curves, which are dependent on the characteristics of the nucleophile and the electrophile, their electronic coupling, and the solvent. At this stage it is not possible predict into what regime a reacting system will fall as evidenced by the two sets of reactions in acetonitrile and dimethyl sulfoxide.

Comparison of Nucleophiles. From the limited data that we have acquired through our picosecond studies, we can begin to examine the relative reactivity of chloride, bromide, and acetate nucleophiles toward the family of diphenylmethyl cations. In comparing reactivities, it is desirable to disentangle kinetics from driving force; this is achieved by examining the reaction dynamics for systems with similar driving forces. For example, in the collapse of the CIP to give rise to R−X, the reaction of the chloride ion with the diphenylmethyl cation has similar driving force in terms of enthalpy, −27.4 kcal/mol, to the reaction of the acetate ion with MethylD+, −27.0 kcal/mol, Figures 6 and 7. The rate constant of the chloride is larger, 3.8×10^9 s^{-1}, than the rate constant of the acetate, 2.2×10^9 s^{-1}. However, the energies of activation for the two processes are the same, $E_a = 3.2$ kcal/mol. It is the difference in the A factors that distinguishes the two rates as the A factor for chloride is a factor of 1.8 larger than the A factor for acetate. Thus, chloride is more reactive than acetate in this comparison, but it is the A factors that are establishing the relative reactivities, not the energies of activation. In contrast, the reaction of bromide with diphenylmethyl cation has a similar enthalpy change, −21.8 kcal/mol, to the reaction acetate with MethoxyD+, −21.3 kcal/mol. The rate of CIP collapse is greater for bromide, 3.2×10^9 s^{-1}, than for acetate, 0.6×10^9 s^{-1}. The factor determining the higher reaction rate for bromide is the lower energy of activation, $E_a = 3.0$ kcal/mol as compared to $E_a = 5.4$ kcal/mol for acetate. From these two examples, in one instance it is the A factor that is controlling relative reactivity while in the other it is the energy of activation that governs relative reactivity. From these initial results, it is doubtful that a simply theory of nucleophilicity can be developed.

Dynamics of Ion-Pair Interconversion. To date, there have been only a limited number of studies examining the dynamics and energetics associated with the interconversion between CIP and SSIP. By examination of the radical ion-pair dynamics of 1,2,4,5-tetracyanobenzene/*p*-xylene, Farid, Goodman, and Gould obtained the free-energy change associated with the conversion of a CIP into a SSIP in a wide range of solvents whose polarity span $\epsilon = 7.2-24.6$.[40] The dependence of the energetics for CIP and SSIP with solvent polarity are well described by the Onsager dipole model and the Born model for ion pairs. In another study, we obtained the activation parameters for the conversion of a CIP into SSIP for *trans*-stilbene/fumaronitrile in a series of alkyl nitrile solvents.[46] Analysis of the activation parameters within the Smoluchowski limit of the Kramers equation gave a good description of the kinetics for radical ion pair diffusional separation.

In discussing the overall reactivity of a nucleophile, account must be taken for the kinetics of the interconversion between ion pairs. From the perspective of free ions reacting, the system must pass through the SSIP into the CIP. For the present series of reactions, the rate of conversion of SSIP into CIP is slower than the collapse of the CIP to form R−X and thus transformation of SSIP into the CIP will make a significant contribution toward determining the overall reactivity. By examination of the reaction profile for chloride reacting with diphenylmethyl cation and acetate reacting with MethylD+ in acetonitrile, the overall energetics for the two systems are similar, which facilitates comparison. The conversion of the chloride SSIP into the CIP occurs with a rate constant of 1.3×10^8 s^{-1}, while the conversion of the acetate SSIP into the CIP occurs with a rate constant of 3.9×10^8 s^{-1}. While rate constant for SSIP → CIP is faster for the acetate, the collapse of CIP giving rise to bond formation is faster for chloride. In another comparison, the conversion SSIP → CIP for MethylD+/acetate in acetonitrile is faster than in dimethyl sulfoxide, and yet the collapse of CIP to give bond formation for MethylD+/acetate is faster in dimethyl sulfoxide than in acetonitrile. From these examples, it is evident that developing models to account for nucleophilicity is going to be challenging.

Comments on the Application of Marcus Equation to the S_N1 Reaction Mechanism. The Marcus equation has found extensive application in the analysis of reaction kinetics in organic chemistry. The analysis has been applied to electron transfer, proton transfer, methyl transfer, as well as nucleophilic addition reactions.[15] Central to the analysis is the determination of the intrinsic reaction barrier obtained by extrapolation of the kinetics for reaction to zero driving force. The importance of an intrinsic barrier is that it allows for the analysis of relative reactivity for a series of reactions at a common driving force.[13] The analysis assumes the standard form of the Marcus equation

$$k = A \exp(-(\lambda + \Delta G)^2/4\lambda RT) \qquad (5)$$

where A is the frequency factor for the reaction, λ the intrinsic barrier, and ΔG the driving force for the reaction. By measurement of k, estimation of ΔG, assumption of an A value of 6.6×10^{12} s^{-1}, the intrinsic barrier is determined.[13] It is important to note that the standard form of the Marcus equation is based within the context of transition-state theory.

(46) Li, B.; Peters, K. S. *J. Phys. Chem.* **1993**, *97*, 7648−7651.

Ritchie has objected to employing the Marcus equation in the analysis of nucleophilic addition reactions.[14] In the original Marcus formulation, the intrinsic barrier is viewed as the average of the intrinsic barriers for two identity reactions.[47] For nucleophilic addition, identity reactions cannot be established. In principle, this definition can be bypassed by assuming that the intrinsic barrier is just the barrier obtained at $\Delta G = 0$. However, to reach this limit the quadratic relationship between the free energy of activation $\Delta G^{\ddagger}$ and ΔG must be assumed. The quadratic relationship is derived by assuming the reactant and product wells are parabolic and have identical curvature.[47] This cannot be the case for a reaction proceeding through a S_N1 mechanism as the reactant and product wells will certainly have different frequencies and anharmonicities reflecting the difference in covalent bonds and ion pairs.[41] How much the $\Delta G^{\ddagger}/\Delta G$ relationship deviates from the quadratic behavior for reactions associated with the S_N1 reaction mechanism has not be established by experiment. However, Hynes theoretical study of the S_N1 reaction mechanism for *tert*-butyl chloride found that the derived intrinsic barrier at zero driving force, employing the Marcus equation, is in error by more than a factor of 2.[41]

The present study raises two further objections to the use of the Marcus equation for the analysis of nucleophilic addition reactions. In its application, the addition reactions are viewed as occurring in a single step, that is, there is one transition state, and the A factor takes on the value obtained from gas-phase transition-state theory, 6.6×10^{12} s^{-1}.[13] The results from the current study reveal that the nucleophile−electrophile recombination passes through at least two transition states associated with SSIP → CIP and CIP → R−X; clearly free ions → SSIP will also be an activated event although it is not kinetically resolved in this work. For the two kinetic events that are resolved, the barriers are comparable to one another and thus one of the events must not be assumed to dominate. Both events should be taken into account, which is not achieved by employing the Marcus equation in form given in eq 5. The second objection in the application of Marcus theory to reactions proceeding through the S_N1 mechanism is that the theory is based on the assumptions of transition-state theory. The effects of polarization caging and nonadiabatic solvation are not taken into account; in other words the κ factor is assumed to be 1.0 in the Marcus equation. If the reaction barriers for covalent bond formation are of the order of 3 kcal/mol or less, then the theory can be in error by more than 1 order of magnitude as we have found a κ factor as small as 0.013 for a barrier of 1.9 kcal/mol.

(47) Marcus, R. A. *J. Phys. Chem.* **1968**, *72*, 891−899.

Conclusions

The above studies reveal important new insights into the parameters that control reactivity for reactions proceeding through the S_N1 reaction mechanism. Organic chemists had originally sought to gain an understanding of S_N1 reactivity through the development of linear free-energy relationships. More recently, the Marcus equation has been employed in the pursuit to ascertain the basis for the variation in nucleophilicity. The present study reveals that for these series of reactions, the dynamics of the underlying processes are more complex than had been originally assumed as a result of the breakdown of transition-state theory. Given that solvent dynamics play a fundamental role in determining passage through the transition state, issues concerning reaction-barrier frequencies, solvent-relaxation times, and solvent frequencies come to the forefront. Line free energy relationships and the Marcus equation cannot capture the essence of the underlying molecular dynamical processes associated with the S_N1 mechanism.

Acknowledgment. This work is supported by a grant from the National Science Foundation, CHE-0408265.

JA051219M